IJPAS | INTERNATIONAL JOURNAL PURE AND APPLIED SCIENCES
ISSN: 2149-0910
Vol. 12(1); 113-132 (2026)
DOI: 10.29132/ijpas.1821773
Research Article

Structural and microstructural evolution of Ag-modified Bi-2212 superconducting ceramics with varying sintering temperatures

Aslı Asiye Ağıl[1,*]

[1]Hakkari University, Department of Materials Science and Engineering, Faculty of Engineering, Hakkari, 30000, Türkiye; asliasiyeagil@hakkari.edu.tr

*Corresponding Author

ARTICLE INFO

Keywords:
Ag addition;
Bi-2212 superconductors;
microstructure evolution;
Williamson–Hall analysis;
sintering temperature.

Dates:
Received: 18 Nov 2025
Accepted: 10 Feb 2026

ABSTRACT

Ag-doped $Bi_2Sr_2CaCu_2O_{8+\delta}$ (Bi-2212) superconducting ceramics were synthesized by the solid-state reaction method and sintered at 835, 840, and 845 °C to examine the effects of Ag addition and sintering temperature on their structural and microstructural characteristics. X-ray diffraction (XRD) confirmed the dominance of the Bi-2212 phase in all samples. Minor changes in the lattice parameters indicated that Ag did not substitute into the crystal lattice, while a slight increase in the *c*-parameter at higher temperatures was attributed to oxygen loss. Williamson–Hall analysis revealed that moderate Ag addition ($x \approx 0.03$) promoted crystallite growth and reduced lattice strain, resulting in a minimum lattice strain energy density. The unit cell volume and *c/a* ratio varied systematically with Ag content and sintering temperature. Scanning electron microscopy (SEM) observations showed that Ag addition up to $x = 0.03$ produced a dense and well-connected microstructure, whereas higher Ag contents ($x \geq 0.05$) and higher temperatures led to Ag-rich segregated regions and localized porosity. These findings demonstrate that Ag does not incorporate into the Bi-2212 lattice but acts as a liquid-phase sintering aid that enhances densification and crystal growth at low levels while causing phase segregation and heterogeneity at high concentrations. The most uniform structure was achieved in the 3 wt.% Ag-doped sample sintered at 840 °C.

1. Introduction

$Bi_2Sr_2CaCu_2O_{8+\delta}$ (Bi-2212), a high-temperature superconductor (HTS), is one of the most researched systems due to its critical temperature (T_c) of approximately 85–95 K and its multilayered crystal structure. The layered structure of Bi-2212 consists of alternating layers of CuO_2 superconducting planes with Bi–O and Sr–O interlayers, and therefore the electrical and structural properties of the material are susceptible to oxygen stoichiometry, phase purity, and microstructural density [1,2]. The properties of Bi-2212 ceramics vary significantly depending on the sintering conditions, additive elements, and processing method.

In the literature, Ag doping stands out as one of the most frequently used modification methods in Bi-2212 systems. Ag addition accelerates the formation of the superconducting phase, facilitates densification by creating a liquid-like environment at grain boundaries, and improves electrical transport pathways [3,4]. However, various studies have indicated that Ag does not directly enter the Bi-2212 lattice as a substitution, but rather that its primary effect is to facilitate the sintering mechanism by increasing diffusion kinetics [5,6]. Ag addition has also been reported to reduce porosity, increase grain size, and strengthen intergranular bonding [7,8]. However, with increasing Ag ratio, adverse effects such as phase separation, oxygen loss, and microstructural heterogeneity may occur [9].

Sintering temperature is another critical parameter that directly affects the structural integrity and oxygen content of Bi-2212. Densification cannot be achieved at low temperatures due to insufficient diffusion, while at high temperatures, oxygen volatilization and anisotropic strain increase (e.g., *c*-axis broadening) dominate the structure [10]. Therefore, the combined evaluation of sintering temperature and Ag doping is of critical importance in terms of both phase formation–densification balance and internal stress–oxygen loss interaction in Bi-2212 systems.

In this study, Bi-2212 ceramics were sintered at 835, 840, and 845 °C after adding different amounts of Ag (x = 0–0.10). The resulting samples were comprehensively characterized using X-ray diffraction (XRD), Rietveld refinement, Williamson–Hall (W–H) analysis, lattice strain energy density calculations, and SEM microstructure images. XRD results revealed how lattice parameters changed with Ag doping and sintering temperature, W–H analysis revealed the relationship between crystallite size and microstrain, and SEM images showed the tendency for microstructural densification. In addition, the effects of Ag doping on the Bi-2212 lattice were investigated quantitatively by evaluating the cell volume ($V = a^2c$), c/a ratio, and elastic energy density ($u = \frac{1}{2}E\varepsilon^2$) values calculated from the obtained data.

2. Materials and Methods

Bulk ceramic samples with compositions of $Bi_{2-x}Ag_xSr_2CaCu_2O_{8+\delta}$ (x = 0, 0.01, 0.03, 0.05, and 0.1) were synthesized using a conventional solid-state reaction method. High-purity Bi_2O_3 (Alfa Aesar, 99%), $SrCO_3$ (Sigma Aldrich, ≥ 98%), $CaCO_3$ (Sigma Aldrich, ≥99%), CuO (Sigma Aldrich, nanopowder), and Ag_2O (Alfa Aesar, 99+%) were used as starting powders.

The powders, weighed in the specified stoichiometric ratios, were homogenized by mixing in a PET bottle using zirconium balls in a ball mill for four hours. The homogeneous mixture was subjected to a three-stage calcination process in an air atmosphere:

15 hours at 800°C,

25 hours at 820°C,

40 hours at 830°C.

After each calcination step, the powders were mixed in the ball mill for 4 hours to increase homogeneity.

Following the calcination process, the resulting powders were pressed under 375 MPa pressure into pellets with a diameter of 13 mm and a thickness of 1 mm. The pellets were sintered in air at temperatures of 835, 840, and 845 °C, respectively, for 60 hours. After the first sintering, the samples were ground into powder in an agate mortar and then pressed again under 650 MPa. After this second pressing, the samples were sintered a second time at the same sintering temperatures (835, 840, and 845 °C, 60 hours). Samples are labeled as (a) A (x = 0), (b) B (x = 0.01), (c) C (x = 0.03), (d) D (x = 0.05), and (e) E (x = 0.10), respectively, according to increasing Ag content.

This multi-stage sintering process was applied to increase phase purity, strengthen intergranular bonding, and improve microstructural densification in the samples.

2.1. Structural and microstructural characterization

The phase composition and structural properties of the samples were determined by X-ray diffraction (XRD) analysis. Measurements were performed on a Rigaku MiniFlex 600 model diffractometer using Cu K_α (λ = 1.5406 Å) radiation at 40 kV and 30 mA. Diffraction patterns were taken in the appropriate 2θ range, and the resulting data were used to determine phase identification and lattice parameters using Rietveld refinement.

Microstructural characterization of the samples was performed with a Zeiss Supra 50 VP scanning electron microscope (SEM). Images were taken in secondary electron (SE) mode at 15 kV accelerating voltage. The obtained micrographs were used to evaluate the grain morphology, densification behavior, and the effects of Ag doping and sintering temperatures on the microstructure.

2.2. Williamson–Hall method

Peak widths obtained from X-ray diffraction (XRD) patterns provide information about the material's crystallite size (D) and the microstrain (ε) within the lattice. The relationship between these two parameters was evaluated using the Williamson–Hall (W–H) method. The W–H approach takes into account the microstrain effect, which is not considered in the Scherrer equation. It separates the peak broadening into two components, both size and strain contributions [11].

This method is based on the following relation:

$$\beta Cos\theta = \frac{k\lambda}{D} + 4\varepsilon Sin\theta \tag{2.1}$$

where β: Full width at half maximum (FWHM, in radians), θ: Bragg diffraction angle, λ: X-ray wavelength (CuK_α, 1.5406 Å), k: Shape factor (taken as 0.9), D: Crystallite size (nm), and ε: Microstrain (dimensionless) value.

In this study, β values were calculated using the six most prominent peaks in the XRD patterns ((008), (115), (0010), (117), (020), and (119)). The resulting FWHM values were converted to radians, and device width correction was applied where necessary. The βcosθ–4sinθ relationship calculated from these data was subjected to linear regression to determine the crystallite size and microstrain values for each sample.

3. Results and Discussion

3.1. XRD analysis and phase formation

Figure 1 shows X-Ray diffraction (XRD) patterns of Ag-modified Bi-2212 ceramic samples sintered at 835 °C, 840 °C, and 845 °C. A (x = 0) represents the pure sample, and samples B (x = 0.01), C (x = 0.03), D (x = 0.05) and E (x = 0.10) represent different Ag doping ratios.

The main reflections observed in all samples belong to the Bi-2212 phase, and the characteristic peaks (00l) (002, 006, 008, 0010) and (hkl) (113, 115, 107, 020, 119, 220, 0210, and 1115) are clearly distinguishable. This result shows that the Bi-2212 phase is dominantly preserved in the sintering temperature range.

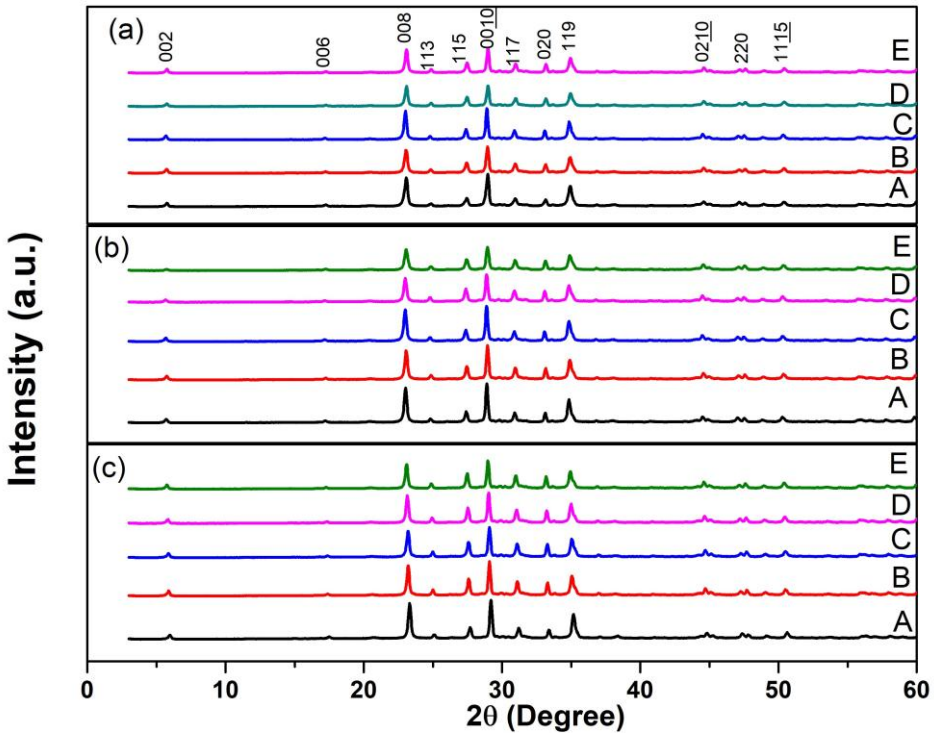


Figure 1. X-ray diffraction patterns of Ag-modified Bi-2212 ceramic samples sintered at (a) 835 °C, (b) 840 °C, and (c) 845 °C. A: x = 0, B: x = 0.01, C: x = 0.03, D: x = 0.05, E: x = 0.10.

Samples sintered at 835°C (Fig. 1(a)):

Although the differences in peak broadening are not visually prominent in the XRD patterns, the Williamson–Hall analysis quantitatively reveals higher microstrain and smaller crystallite sizes at lower sintering temperatures. Low-intensity Bi-2201 side-phase reflections are observed in some samples. As the Ag content increases, a slight increase in the intensity of the (B–E) (00l) peaks and a decreasing trend in full-width half maximum (FWHM) values are observed. This suggests that Ag facilitates grain growth by accelerating the sintering kinetics at this temperature.

Samples sintered at 840 °C (Fig. 1(b)):

The peaks appear to have sharpened significantly and their intensities have increased, indicating a higher degree of crystallinity and reduced microstrain. Additionally, the weak reflections of the Bi-2201 phase have largely disappeared. It is observed that phase purity and crystalline order improve with increasing Ag doping. This temperature can be considered the optimum sintering temperature for the formation of the Bi-2212 phase.

Samples sintered at 845 °C (Fig. 1 (c)):

The enhancement in crystallization was evaluated quantitatively through XRD-based Williamson–Hall analysis and Rietveld refinement results. The observed increase in crystallite size, accompanied by a reduction in lattice microstrain and more stable lattice parameters, indicates improved crystallinity rather than changes inferred from visual inspection of peak intensities. Additionally, a significant increase in the intensity of the (00l) peaks suggests that the grains are oriented parallel to the *c*-axis (texture formation). In sample E with the highest Ag content, metallic Ag (111) and (200) reflections became

prominent around $2\theta \approx 38°$ and 44°, indicating that Ag did not wholly penetrate the lattice but remained largely as a separate metallic phase.

As a result, the dominant phase at all temperatures is Bi-2212, with only traces of 2201 or 2223 phases present. At 840 °C, the most stable structure was achieved in terms of crystallinity, phase purity, and grain connectivity. The Ag additive does not significantly penetrate the lattice, but instead resides primarily at grain boundaries or in micropores, increasing sintering efficiency through its wetting effect. The texture trend observed at 845 °C, combined with long sintering time, results in grain orientation and high crystal quality.

These findings are consistent with similar studies in the literature; for example, studies on Bi-2212/Ag tape and ceramic systems show that Ag doping exhibits liquid-phase-like behavior at grain boundaries, increasing grain connectivity and facilitating grain growth [7,8]. This increase is also reported in the literature to occur without any significant substitution effect in the lattice parameters.

Although Ag exhibits a liquid-like behavior at the applied sintering temperatures, the present results indicate that the sintering mechanism does not correspond to classical liquid-phase sintering involving dissolution, transport, and reprecipitation of matrix ions. XRD patterns and Rietveld refinement results show no evidence of Ag incorporation into the Bi-2212 lattice, indicating negligible chemical solubility of Bi-2212 constituents in Ag. Instead, Ag acts as a transient metallic liquid phase that promotes densification mainly through particle rearrangement, grain-boundary wetting, capillary forces, and enhanced grain-boundary diffusion. SEM observations further confirm this interpretation by showing improved grain connectivity at moderate Ag contents, while higher Ag additions result in segregated Ag-rich regions rather than homogeneous solid solutions. Therefore, the role of Ag in this system is more accurately described as a liquid-phase-assisted sintering aid rather than a classical solution–precipitation-based liquid-phase sintering mechanism.

3.2. Lattice parameters (Rietveld refinement)

Table 1 shows the lattice parameters obtained from the Rietveld refinement of Ag-modified Bi-2212 ceramics sintered at 835, 840, and 845 °C according to the tetragonal unit cell (I4/mmm). The Bi-2212 phase was dominant in all samples, and limited changes were observed in the *a* and *c* axes depending on the Ag doping.

At 835 °C, the *a* parameter varies between 5.432 Å (A) and 5.443 Å (C), while the *c* parameter is in the range of 30.76–30.83 Å. Particularly in sample C (x = 0.03), the slight increase observed along both axes suggests that the low amount of Ag doping partially compensates for oxygen vacancies in the crystal lattice, thus slightly widening the interlayer distance (*c*). At higher Ag ratios (D–E), the parameters decrease again, supporting that Ag remains mainly as a separate phase at the grain boundaries.

In samples sintered at 840 °C, $a \approx 5.434$–5.445 Å and $c \approx 30.76$–30.89 Å were observed, with the highest value observed in sample C (x = 0.03). Considering the sharp peaks and low refinement errors, 840 °C can be regarded as the optimum crystallization temperature. Ag addition slightly increases *a* and *c* in the 0.01–0.03 range, indicating more homogeneous intragranular diffusion and oxygenation. At higher Ag ratios, the parameters become smaller again, indicating that the internal stress in the lattice partially increases.

Table 1. Change of lattice parameters *a* and *c* according to Ag doping ratio (separate series for each temperature).

Sintering Temperature (°C)	Sample	a-axis lattice parameter (Å)	c-axis lattice parameter (Å)
835	A	5.4322	30.7959
	B	5.4351	30.7787
	C	5.4430	30.8336
	D	5.4328	30.7647
	E	5.4315	30.7791
840	A	5.4443	30.8562
	B	5.4376	30.7926
	C	5.4454	30.8946
	D	5.4384	30.7738
	E	5.4339	30.7648
845	A	5.4044	30.6204
	B	5.3886	30.7786
	C	5.3915	30.7713
	D	5.3962	30.8144
	E	5.4019	30.8502

A significant decrease in the *a* parameter (to around 5.40 Å) is observed at 845 °C. This decrease can be attributed to oxygen loss and unit cell shrinkage due to Bi volatility at high temperatures. The relative stability of the *c*-axis in samples C and D indicates that the anisotropy in the layered structure is preserved. In addition, the increase in the intensity of the peaks at high temperature (00l) (see Fig. 1) explains this change with the effect of texturing (preferred orientation).

As a result, the *a* and *c* parameters showed small (< 0.2%) oscillations depending on the sintering temperature and Ag content. The most regular and stable values were obtained at 840 °C; it can be said that the crystal structure developed best at this temperature. It is believed that Ag is not incorporated into the lattice substitutionally, and the limited change in parameters is primarily due to oxygen stoichiometry and texture effects. The cell volume ($V = a^2c$) tends to increase slightly from 835 °C to 840 °C and to decrease at 845 °C, indicating a structural tendency towards first crystallization and then partial oxygen loss.

This behavior is consistent with results reported in the literature. For example, studies on Ag-doped Bi-2212 systems indicate that Ag enhances grain connectivity and facilitates crystallization through

liquid-phase-like interactions at grain boundaries [12-14]. However, it is also reported in the literature that this improvement does not lead to a significant substitutional change in the lattice parameters.

3.3. Crystallite size and microstrain analysis

Fig. 2 (a–c) shows the changes in crystallite size (D) and microstrain (ε) values obtained depending on Ag addition at different sintering temperatures (835, 840, and 845 °C). The relevant numerical data are summarized in Table 2. It is observed that Ag doping has significant effects on the microstructural integrity of the crystal structure at all three temperatures.

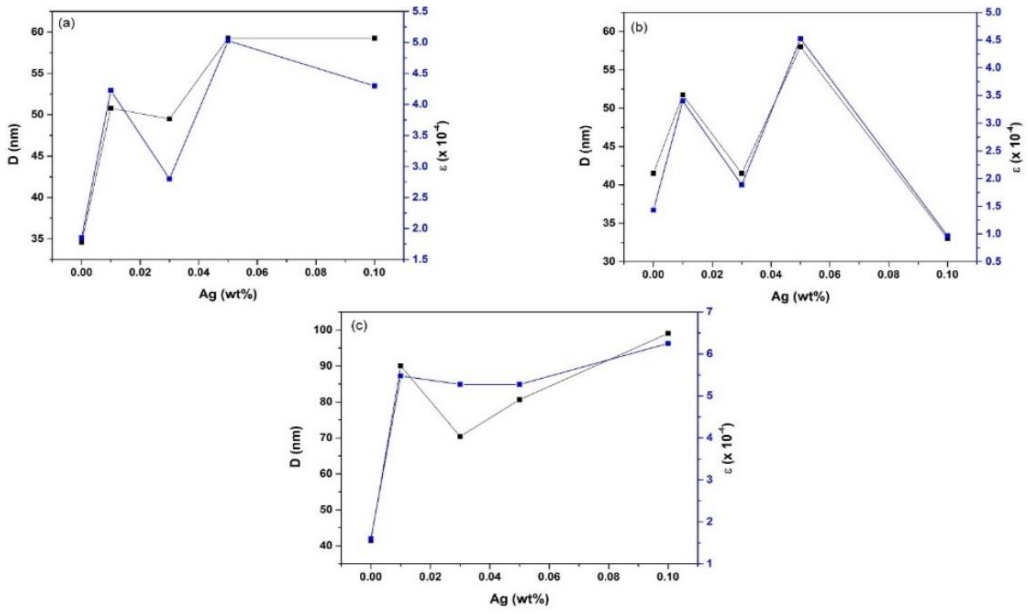


Figure 2. Changes in crystallite size (D) and microstrain (ε) values of Ag-modified Bi-2212 ceramics sintered at (a) 835 °C, (b) 840 °C, and (c) 845 °C depending on the Ag doping ratio.

Samples sintered at 835 °C (Fig. 2 (a)):

The sample (A) without Ag additives had the smallest crystallite size (34.6 nm). When the Ag content was increased to x = 0.01, the crystallite size increased significantly, reaching 50.8 nm. This increase is due to Ag's wetting effect at grain boundaries during sintering, facilitating atomic diffusion. While the Ag doping was stabilized in the x = 0.03–0.10 range, the crystallite size stabilized at approximately 49–59 nm, and microstrain values increased from 1.8 $\times 10^{-4}$ to 5.0 $\times 10^{-4}$. This suggests that Ag can promote crystal growth while simultaneously causing an increase in partial strain. This behavior is consistent with similar studies in the literature. For example, Díez et al. [15] and Atilla et al. [16] reported that Ag doping facilitates crystallization and strengthens intergrain connections by creating a liquid phase-like effect at the grain boundaries in Bi-2212 systems.

Table 2. Crystallite size and microstrain values obtained from Williamson–Hall analysis of Ag-doped Bi-2212 samples sintered in the range of 835–845 °C.

Sintering Temperature (°C)	Sample	D (nm)	ε (x 10^{-4}) (dimensionless)
835	A	34.57	1.85
	B	50.78	4.22
	C	49.51	2.80
	D	59.25	5.02
	E	59.25	4.30
840	A	41.51	1.43
	B	51.73	3.40
	C	41.51	1.88
	D	58.01	4.52
	E	33.01	0.96
845	A	41.38	1.60
	B	90.03	5.47
	C	70.38	5.27
	D	80.61	5.27
	E	99.03	6.25

Samples sintered at 840 °C (Fig. 2 (b)):

As the sintering temperature increased, crystallinity increased, resulting in an overall increase in crystallite size. Ag doping yielded the highest *D* value (58.0 nm) at 0.05 wt%. However, at higher Ag ratios (x = 0.10), a decrease in size (33.0 nm) and strain (0.96 $\times 10^{-4}$) was observed. This decrease can be attributed to the separation of Ag into a separate phase at high temperatures and the formation of a molten metallic film at grain boundaries. Indeed, it has been reported that the addition of Ag in Bi-2212/Ag systems reduces the melting temperature by forming a melt-like (eutectic) intermediate phase, facilitates grain growth/texturization, and improves inter-grain bonding [17].

Samples sintered at 845 °C (Fig. 2 (c)):

At the highest sintering temperature, crystallite sizes increased significantly. The sample (E) with Ag doping at x = 0.10 yielded the highest value in the entire series, with a crystallite size of approximately 99 nm. At this temperature, the liquid phase sintering mechanism was activated due to the low melting point of Ag, which accelerated grain growth. In contrast, microstrain values increased from 1.6 $\times 10^{-4}$ to 6.3 $\times 10^{-4}$, indicating that intra-lattice defects did not wholly disappear despite increased grain growth. Such a 'dual effect' has also been reported in laser-floating zone (LFZ) and tape/ribbon processing studies in Bi-2212/Ag systems: While Ag addition accelerates grain growth and texturing by

creating a melt-like interphase, strain/defect contributions to line broadening may not be eliminated during processing (see [9,18]). Simultaneous diffraction findings regarding the evolution of the structure during heat treatment are also consistent with this table [19].

As a general result, crystallite sizes ranged from approximately 35–99 nm between 835–845 °C. Increasing Ag doping increased grain growth and crystallization, particularly at low and medium temperatures, while at high temperatures, it caused instability due to phase separation. Microstrain values are generally on the order of 10^{-4} and tend to increase with increasing sintering temperature. These trends support the view that Ag does not directly enter the Bi-2212 lattice but instead locates at the grain boundaries, facilitating diffusion and condensation.

3.4. Cell volume and anisotropy (*c/a*) change in Ag-modified Bi-2212 ceramics

Fig. 3 shows the changes in cell volume ($V = a^2c$) and *c/a* ratio of Ag-modified Bi-2212 ceramics sintered at various temperatures depending on the Ag doping ratio. The data were calculated from the lattice parameters obtained from the Rietveld refinement.

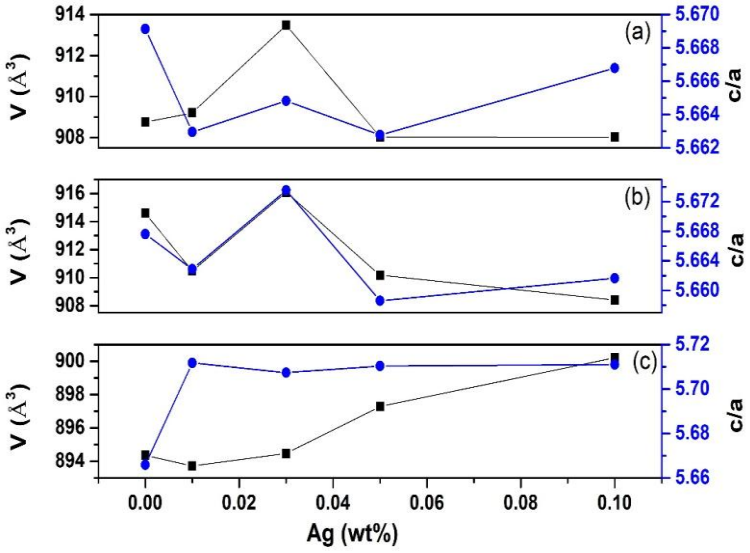


Figure 3. Changes in cell volume ($V = a^2c$) and *c/a* ratio of Ag-modified Bi-2212 ceramics sintered at (a) 835 °C, (b) 840 °C, and (c) 845 °C depending on the Ag doping ratio.

Among samples sintered at 835 °C, the Ag-free sample had the lowest cell volume (≈ 909 Å³), while $V \approx 913$ Å³ was reached with low Ag doping (x = 0.03). This increase is due to Ag's wetting effect at grain boundaries during sintering, facilitating densification. The slight increase in the *c/a* ratio at the same doping ratio indicates that interlayer order improved with crystallization. As the Ag ratio increased to higher values ($x \geq 0.05$), the volume tended to decrease again, suggesting that Ag began to form separate metallic phases rather than contributing to the lattice. This trend is consistent with the increase in crystallite size (35 → 60 nm) and the fact that microstrain remains low (order of 10^{-4}) in W–H analysis.

The cell volume generally increased slightly at 840 °C ($V \approx 909$–915 Å³). In particular, the volume reached a maximum at the x = 0.03 doping and then decreased again. This indicates that the sintering

temperature is the optimum condition that balances crystallinity and oxygen diffusion. The change in the *c/a* ratio is quite limited (5.660–5.672). This stability supports the notion that the Ag doping is not substitutionally incorporated into the Bi-2212 lattice and therefore does not significantly affect crystal anisotropy.

At the highest sintering temperature used in this study, a significant decrease in cell volume (≈ 894–900 Å³) is observed. This decrease is associated with a reduction in the *a*-parameter due to oxygen loss at high temperatures. In contrast, the *c/a* ratio (5.66 → 5.72) increased, indicating a strengthening of the interlayer spacing and texture formation trend. The intensification of the peaks at high temperatures (00l) in the XRD patterns also supports this trend. This trend was observed at 845 °C, combined with the high crystallite size (≈ 90–100 nm) obtained in W–H analysis, but the fact that microstrain does not entirely disappear indicates a partially relaxed but not fully homogeneous crystal lattice. Similarly, Matsumoto et al. reported that Ag exhibits liquid-phase-like behavior at high temperatures, increasing grain growth, but cannot fully preserve oxygen stoichiometry [9].

Consequently, Ag addition promoted crystallization and densification at low to moderate concentrations (x ≤ 0.05), reflected in an increase in *V* and a slight increase in *c/a*. At high temperature (845 °C), oxygen loss and texture effects became dominant; as *V* decreased, an increase in *c/a* increased structural anisotropy. This behavior supports the dominance of the Bi-2212 phase observed in XRD phase analyses and the balance between crystallite size and microgranularity in W–H analyses. It is understood that Ag does not enter the lattice directly but rather affects the sintering kinetics by localizing mainly at grain boundaries and microvoids.

3.5. Lattice strain energy density (*u*)

Using the microstrain (ε) values obtained from the Williamson–Hall analysis, the elastic energy density (u) stored in the lattice was calculated with the following relationship:

$$u = \frac{1}{2} E \varepsilon^2 \tag{3.1}$$

where E is the average Young's modulus reported in the literature for Bi-2212 ceramics. In the literature, elastic modulus measurements for Bi-2212 ceramics are reported in the range of 48–70 GPa [20]; in this study, $E \approx 130$ GPa was accepted since the crystal density and sintering conditions were relatively high.

Fig. 4 presents the lattice strain energy density values calculated at different sintering temperatures depending on the Ag doping ratio. At 835 ºC, the sample (A) without Ag doping had the lowest energy density (~2 × 10^3 J m^{-3}). With the addition of 1 wt% Ag, the u value increased to ~11 × 10^3 J m^{-3}, followed by a slight decrease at medium inclusions and a re-increase at high inclusions (x = 0.1). This fluctuating trend suggests that Ag initially reduces internal stresses by facilitating diffusion at grain boundaries, while at higher rates it creates local elastic energy zones through microsegregation. This trend is consistent with the increase in crystallite size (35 → 60 nm) and limited rise in microstrain observed in W–H analysis.

At 840 °C, u values generally remained in the range of 0–12 × 10^3 J m^{-3}. This low energy density reflects optimal sintering conditions where crystallization and oxygen diffusion are balanced. The lowest

values of u in this series coincide with the smallest microstrains observed in the W–H analysis ($\varepsilon \approx 2 \times 10^{-4}$). Therefore, 840 °C indicates the most stable crystal lattice in terms of both microstrain and energy density.

At 845 °C, u values increased significantly (~20–25 × 10^3 J m^{-3}). This increase is associated with an increase in ε due to oxygen loss at high temperature and anisotropic texturing. The liquid-phase-like behavior of Ag promotes grain growth, but strains are not eliminated.

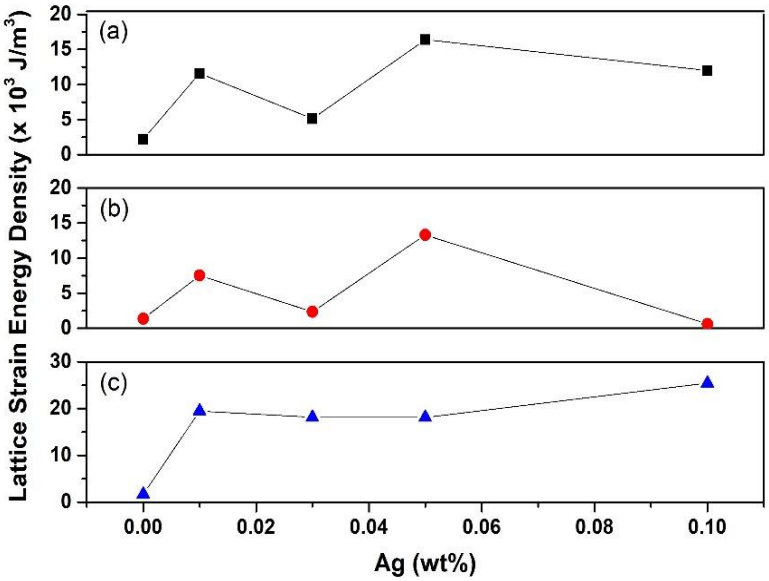


Figure 4. Lattice strain energy density as a function of Ag content for Bi-2212 ceramics sintered at (a) 835 °C, (b) 840 °C, and (c) 845 °C. The values are plotted in units of 10^3 J m^{-3}.

3.6. Microstructural analysis of Ag-modified Bi-2212 ceramics

It should be emphasized that the influence of sintering temperature on densification discussed in this study is inferred from qualitative SEM observations, including grain connectivity and pore evolution, rather than from direct bulk density measurements. Therefore, SEM images are used as indirect indicators of densification behavior without implying a quantitative correlation with bulk density values.

Fig. 5 shows SEM images (A–E) of Ag-modified Bi-2212 ceramics sintered at 835 °C. In Ag-free sample A, the microstructure is highly porous, and the grains exhibit a fine, irregular morphology. The weak grain connectivity and distinct boundaries indicate that 835 °C was not sufficient for complete condensation of the Bi-2212 phase. This structure is consistent with the low phase ratio seen in XRD analysis and the small crystallite sizes (~35 nm) obtained from Williamson–Hall analysis.

Lower-magnification images were also evaluated; however, at lower magnifications the characteristic grain morphology and intergranular connectivity of the Bi-2212 ceramics could not be clearly resolved. Therefore, the selected magnification was retained to better capture grain-scale features relevant to densification and microstructural evolution.

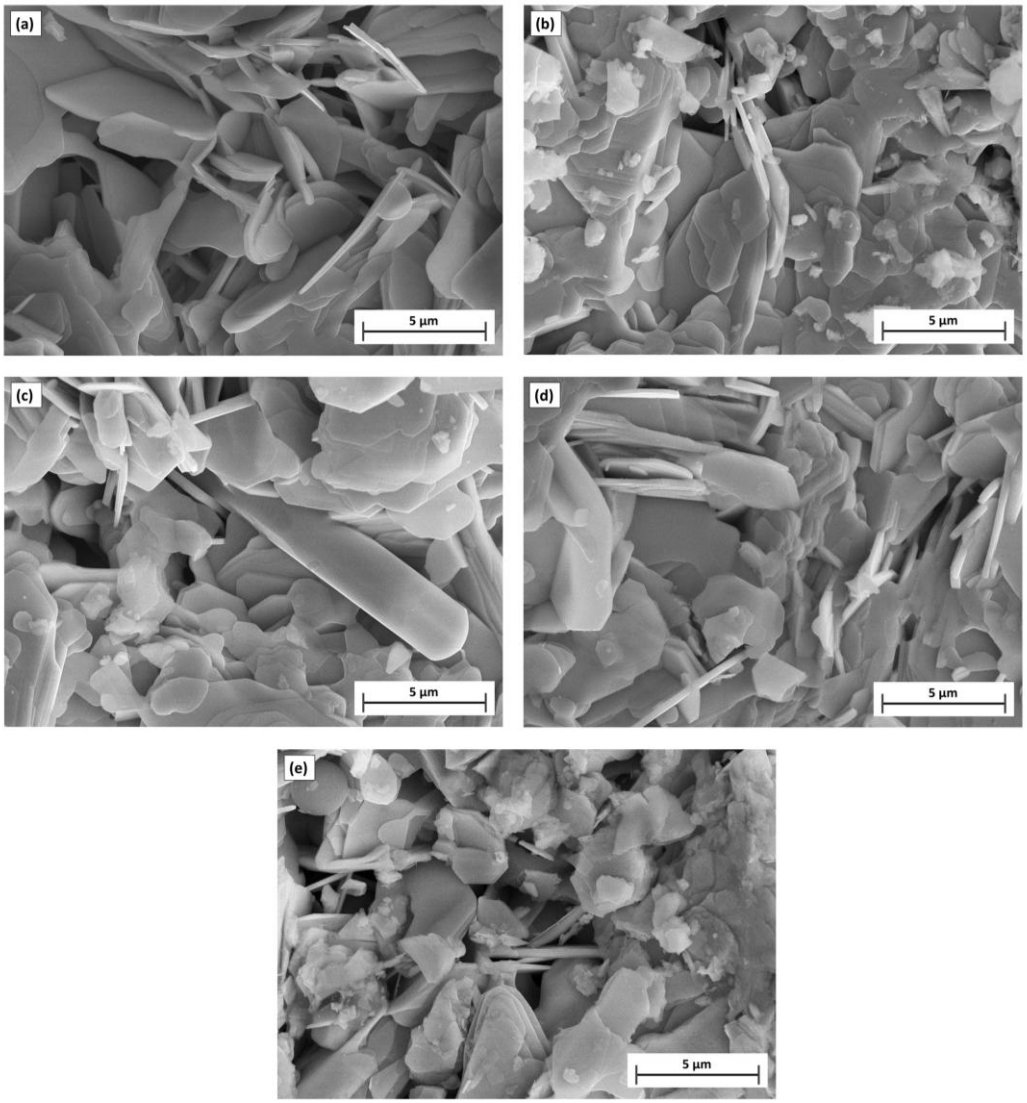


Figure 5. SEM images of Ag-modified Bi-2212 ceramics sintered at 835 °C: (a) A (x = 0), (b) B (x = 0.01), (c) C (x = 0.03), (d) D (x = 0.05), and (e) E (x = 0.10).

A significant improvement in microdensity was observed with the initiation of Ag doping. In sample B (x = 0.01), grains have grown larger, porosity has decreased, and tighter connections have formed. This change is due to Ag's wetting effect at grain boundaries, accelerating diffusion and sintering kinetics. This effect is most pronounced in sample C (x = 0.03); a coarse, plate-shaped intergranular network structure is observed, and the structure becomes more homogeneous. This composition is the one with the highest crystallite size (~60 nm) and lowest microstrain in W–H analysis; therefore, it can be considered as the optimum additive ratio in terms of microstructural density.

When the Ag content reached $x \geq 0.05$ (samples D and E), increased microstructural non-uniformity was observed in the SEM images, accompanied by the reappearance of local porosity. SEM images show Ag phases separated as bright regions and metallic islands on the surface. This separation is consistent with an increase in lattice strain energy density. Although these phases, located at grain

boundaries at high Ag ratios, maintain the connection to some extent, they lead to an increase in microstrain by limiting oxygen diffusion.

In general, at 835 °C, low and moderate Ag doping ($x \leq 0.03$) promoted densification and grain growth in the Bi-2212 phase, while high doping tended to induce phase separation and localized stress accumulation. These observations, consistent with XRD and W–H analyses, suggest that Ag is not incorporated into the lattice substitutionally; its main effect is to control grain boundary diffusion and microstructural connectivity during sintering.

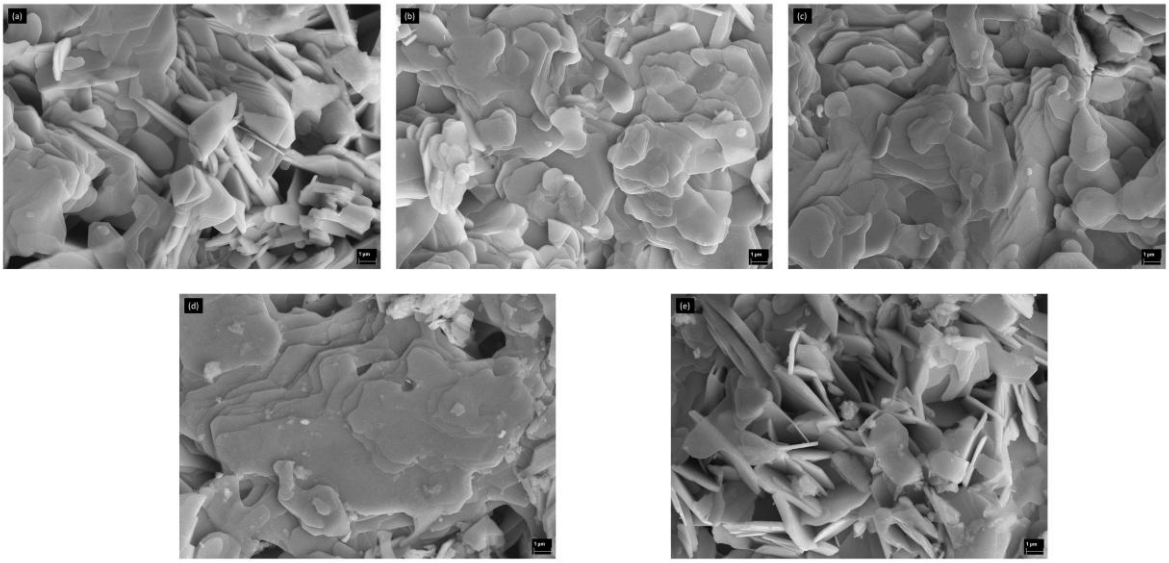


Figure 6. SEM images of Ag-modified Bi-2212 ceramics sintered at 840 °C: (a) A (x = 0), (b) B (x = 0.01), (c) C (x = 0.03), (d) D (x = 0.05), and (e) E (x = 0.10).

Fig. 6 shows SEM images (A–E) of Ag-modified Bi-2212 ceramics sintered at 840 °C. A significant increase in densification was observed in the Ag-free sample A compared to the 835 °C series. Porosity decreased, and grains transformed into a more uniform plate-like morphology. This indicates that a sintering temperature of 840 °C provides optimal crystallization conditions for the Bi-2212 phase. The increase in phase purity in XRD analysis and the increase in crystallite sizes (~50 nm) in W–H analysis support this microstructural development.

With the addition of Ag (samples B and C, x = 0.01–0.03), intergrain boundaries almost disappeared, and a dense, well-connected texture was formed. In these compositions, Ag accelerated grain coalescence and reduced residual stresses in the structure during sintering through its wetting and diffusion-facilitating effects. Grain sizes reached micrometer scales, while porosity was minimized. These observations are consistent with the decrease in microstrain to a minimum ($\varepsilon \approx 2 \times 10^{-4}$) and the low u (elastic energy density) values in the W–H analysis. These results are consistent with the grain growth accelerating effects of Ag reported by Zhang et al. and Chen et al. [21,22].

When the Ag content was $x \geq 0.05$ (samples D and E), signs of local heterogeneity and microroughening appeared in the structure. Particularly in sample E, metallic Ag phases are observed to separate into bright areas on the surface. Although these regions partially protect intergrain connections,

they may inhibit oxygen diffusion, leading to microstrain accumulation. Similarly, Shin et al. reported that high Ag ratios lead to phase segregation and reduce microstructural homogeneity [23].

In general, sintering at 840 °C can be considered the optimal temperature for both crystallization and microstructural bonding. Low to moderate Ag doping ($x \leq 0.03$) facilitated intergranular diffusion, creating a dense and homogeneous structure, while high Ag content ($x \geq 0.05$) increased the tendency for phase separation and local stress accumulation. These observations, consistent with XRD and W–H analyses, indicate that Ag does not enter the Bi-2212 lattice substitutionally, but instead acts as an auxiliary phase controlling the sintering kinetics and grain connectivity.

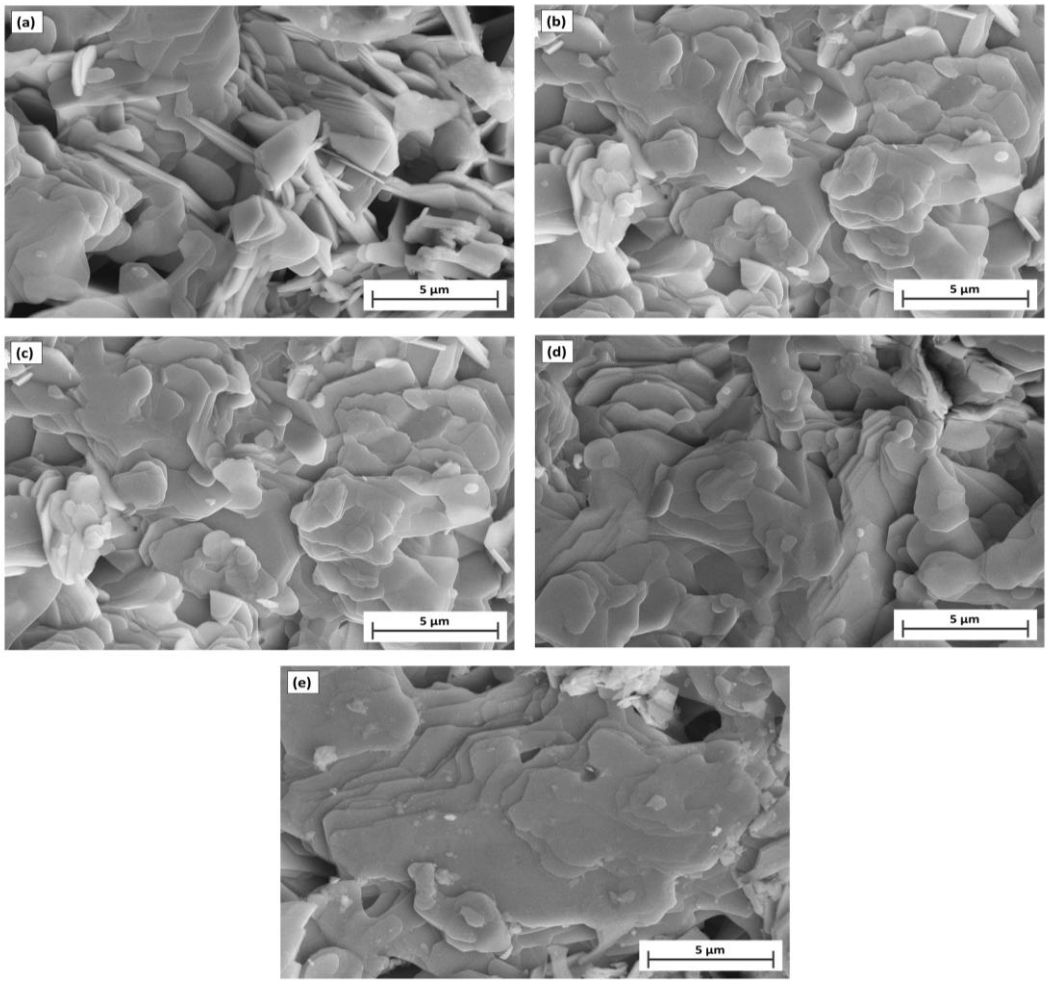


Figure 7. SEM images of Ag-modified Bi-2212 ceramics sintered at 845 °C: (a) A (x = 0), (b) B (x = 0.01), (c) C (x = 0.03), (d) D (x = 0.05), and (e) E (x = 0.10).

Fig. 7 shows SEM images (A–E) of Ag-modified Bi-2212 ceramics sintered at 845 °C. In sample A (x = 0), which does not contain Ag, the grains are larger and more rounded, exhibiting a denser microstructure compared to those at 835 °C and 840 °C. This is related to the acceleration of diffusion at high temperatures, indicating that the Bi-2212 phase is approaching complete crystallization. However, microscopic cracks and a small number of voids are observed in some regions, suggesting that oxygen

volatility has begun to increase. The increase in ε and the increase in u value at this temperature in the Williamson–Hall analysis support this interpretation.

With the initiation of Ag addition (samples B and C, x = 0.01–0.03), the structure attained a smoother and more compact morphology. Molten-phase-like connections formed between the grains, and porosity decreased significantly. This can be explained by the initiation of a liquid-phase sintering mechanism due to the low melting point of Ag. Thus, diffusion at grain boundaries accelerated, partially relieving microstrain. This behavior was also reported in the studies of Kahraman et al. and Matsumoto et al. [7,9].

At Ag contents of $x \geq 0.05$ (samples D and E), surface regions exhibiting morphological contrast variations and bright Ag-rich features became apparent in the SEM micrographs. These metallic phases partially melt during sintering, accumulating at grain boundaries and forming local liquid-phase pockets. Thus, although the bonding improves in some regions, oxygen diffusion is restricted in others, and microstrain increases again. This phase separation is consistent with the increased anisotropy observed in cell volume-c/a analyses. Similarly, Zhang et al. reported that Ag doping at high temperature disrupted the oxygen balance and created microstructural heterogeneity [21].

In general, sintering at 845 °C resulted in maximum crystallization and grain growth in the Bi-2212 phase; however, increasing the Ag content, while facilitating bonding, also increased internal stresses due to phase segregation and oxygen loss. Therefore, optimal microstructural homogeneity and low strain energy are achieved around 840 °C and at an additive ratio of $x \approx 0.03$. These observations, when evaluated together with previous XRD, W-H and lattice strain energy density results, clearly reveal that Ag is not directly incorporated into the lattice but regulates the diffusion kinetics as an auxiliary phase during the sintering process.

Although elemental mapping by EDS could provide additional insight into the spatial distribution of Ag, such analysis could not be performed within the scope of the present study. Nevertheless, the absence of Ag-related lattice distortions in XRD/Rietveld results, together with the observation of Ag-rich segregated regions in SEM images at higher Ag contents, consistently indicates that Ag remains primarily at grain boundaries rather than being incorporated into the Bi-2212 lattice.It should be noted that direct bulk density measurements could not be performed for the present samples due to experimental limitations. Therefore, the discussion of densification in this study is based on indirect structural and microstructural indicators, including SEM observations, crystallite size evolution, microstrain, and lattice strain energy density derived from XRD analyses.

As summarized in Table 3, previous studies mainly focused on either Ag addition or processing conditions independently. In contrast, the present study systematically correlates Ag content and sintering temperature with crystallite growth, lattice strain, and lattice parameter evolution. The identification of an optimal Ag content ($x \approx 0.03$) associated with enhanced crystallite growth and reduced microstrain distinguishes this work from earlier reports, which primarily emphasized microstructural or superconducting properties.

Table 3. Comparison of crystallite growth and lattice parameter evolution in Ag-modified Bi-2212 ceramics

Reference	**Material system**	**Additive (type and amount)**	**Sintering/ Processing conditions**	**Lattice parameters (trend)**	**Crystallite growth / microstructural observation**	**Key remarks**
This work	$Bi_2Sr_2CaCu_2O_{8+\delta}$	Ag, x = 0–0.10	Solid-state reaction; 835, 840, 845 °C	a ≈ constant, c slightly increases at higher T	Crystallite size increases and microstrain decreases at x ≈ 0.03; higher Ag causes non-uniformity	Systematic correlation of Ag content and sintering Temperature using W–H and Rietveld analyses
[8]	Bi-2212	Metallic Ag (various	Conventional ceramic processing	Minor lattice parameter changes; no clear Ag	Improved microstructure at low Ag contents	Ag mainly affects microstructure rather than crystal lattice
[7]	Bi-2212/Ag composite	Ag (hot-pressed)	Hot-pressing, 800–850 °C	Lattice parameters not strongly modified	Larger grains, improved connectivity, reduced secondary phases	Densification enhanced by Ag-assisted processing
[24]	Bi-based cuprate with Ag	Ag-containing compositions	Post-annealing treatments	Lattice parameters sensitive to thermal treatment	Microstructural improvement correlated with annealing	Highlights role of thermal history
[17]	Bi-2212 textured rods with Ag	Ag addition	Floating-zone texturing	No evidence of Ag lattice in-corporation	Grain alignment and microstructural refinement	Ag acts as a processing aid
[25]	Bi-2212 with Ag substitution attempts	Ag at Bi/Sr/Cu sites	Controlled cooling regimes	c-axis varies with oxygenation and cooling rate	Structural response linked to oxygen content	Emphasizes oxygen-driven lattice changes

4. Conclusion

$Bi_2Sr_2CaCu_2O_{8+\delta}$ (Bi-2212) superconducting ceramics containing varying amounts of Ag were successfully synthesized at 835, 840, and 845 °C to determine the effects of Ag doping and sintering temperature on structural evolution. X-ray diffraction (XRD) analyses revealed that Bi-2212 was the dominant phase in all samples. Small changes in lattice parameters indicate that Ag does not penetrate the crystal lattice but rather exerts its primary influence at grain boundaries. According to the Rietveld refinement results, the *a*-parameter remained essentially constant, while the *c*-parameter and cell volume increased slightly with temperature. This can be explained by the partial oxygen loss and the resulting lattice expansion at high temperatures.

Data from Williamson–Hall analysis revealed that moderate Ag doping ($x \approx 0.03$) promotes crystallite growth and reduces lattice strain. The calculated lattice strain energy density for this composition reached a minimum. This result suggests that limited Ag addition reduces internal stresses and facilitates structural relaxation. In contrast, higher Ag ratios and increased sintering temperature caused an increase in microstrain and elastic energy density due to oxygen volatilization and anisotropic distortion in the lattice.

SEM studies supported the findings from diffraction analyses. Increasing the Ag content up to $x = 0.03$ resulted in a dense and homogeneous microstructure with tightly packed grains. However, at higher Ag concentrations, SEM observations revealed the formation of Ag-rich surface features and local porosity, leading to increased microstructural non-uniformity. This indicates that Ag is not directly incorporated into the lattice but acts mainly as an auxiliary phase that facilitates liquid-phase sintering.

As a result, the sample sintered at 840 °C and containing 3 wt% Ag exhibited optimal structural properties, with the most homogeneous microstructure, lowest internal stress, and most stable lattice parameters. This study provides essential data for optimizing the fabrication conditions of Bi-based superconducting ceramics by revealing that Ag doping plays a role in regulating microstructural diffusion and densification in Bi-2212 systems rather than direct chemical doping.

Acknowledgement

The author would like to express their sincere gratitude to the reviewers and editorial board of the *International Journal of Pure and Applied Sciences* for their valuable comments and constructive suggestions that helped improve the quality of this manuscript.

Conflict of Interest

The author declare that there is no conflict of interest regarding the publication of this paper. The study was written with the contribution and approval of all authors.

Research and Publication Ethics Statement

The author declare that all procedures in this study were carried out in accordance with the scientific, ethical, and citation principles of the *International Journal of Pure and Applied Sciences*. The author confirm that they have complied with all ethical guidelines of the journal throughout the research and publication process.

References

[1] M. Vallet-Regi, A. Caneiro, J. M. Gonzalez-Calbet, J. Ramirez, C. Rillo, A. Badia, L. A. Angurel, F. Lera, R. Navarro, "Influence of oxygen stoichiometry on T_c and pinning force of $Bi_2Sr_2CaCu_2O_{8+\delta}$", *Physica C: Superconductivity,* vol. 185-189, part 4, pp. 2475-2476, Dec 1991, doi:10.1016/0921-4534(91)91362-8.

[2] T. W. Li, P. H. Kes, W. T. Fu, A. A. Menovsky, J. J. M. Franse, "Anisotropic oxygen diffusion in $Bi_2Sr_2CaCu_2O_{8+x}$ single crystals", *Physica C: Superconductivity*, vol. 224, pp. 110-116, Apr 1994, doi:10.1016/0921-4534(94)90611-4.

[3] H. Najafpour, S. H. R. Shojaei, S. M. Shojaei, "The Effect of $AgNO_3$ Addition on the Formation and Superconducting Properties of the Bi2223 Phase", *J. Supercond. Nov. Magn.*, 23, pp. 487–491, May 2010, doi:10.1007/s10948-009-0603-5.

[4] Y. Nakamura, T. Tsukamoto, K. Koyama, S. Noguchi, "Effect of Ag Addition on the Crystal Growth in Bi Cuprate Superconductors", *Materials Transactions JIM*, vol. 33, issue 5, pp. 525-528, May 1992, doi:10.2320/matertrans1989.33.525.

[5] N. K. Man, N. D. Hoa, D. T. T. Nhan, "Improvement of Critical Current Density in Bi-2223 Superconductor by Ag-Doping", *VNU Journal of Science: Mathematics – Physics*, vol. 35, issue 4, pp. 41-51, Dec 2019, doi:10.25073/2588-1124/vnumap.4357.

[6] B. Cevizci, O. Bilgili, K. Kocabas, "The influence of Ag substitution on structural and mechanical properties of (Bi, Pb)-2223 ceramics*", J. Mater. Sci.: Mater. Electron.*, vol. 27, pp. 13171–13178, Dec 2016, doi:10.1007/s10854-016-5463-8.

[7] F. Kahraman, A. Sotelo, M. A. Madre, J. C. Diez, B. Ozkurt, Sh. Rasekh, "Relationship between microstructure and superconducting properties in hot-pressed Bi-2212/Ag ceramic composites", *Ceramics International*, vol. 41, issue 10, pp. 14924-14929, Dec 2015, doi:10.1016/j.ceramint.2015.08.029.

[8] B. Ozkurt, M. A. Madre, A. Sotelo, J. C. Diez, "Effect of metallic Ag on the properties of Bi-2212 ceramic superconductors", *J. Mater. Sci.: Mater. Electron.*, vol. 24, pp. 3344–3351, Sep 2013, doi:10.1007/s10854-013-1253-8.

[9] A. Matsumoto, H. Kitaguchi, H. Kumakura, K. Togano, "The microstructure changes of Bi-2212/Ag composite tapes processed under a temperature gradient", *Physica C: Superconductivity*, vol. 372–376, pp. 913-915, Aug 2002, doi:10.1016/S0921-4534(02)00930-9.

[10] Q. B. Hao, C. S. Li, S. N. Zhang, J. Q. Feng, M. H. Du, "Effect of oxygen partial pressure on the superconductivity of Bi-2212 wires during post-annealing", *Physica C: Superconductivity and its Applications*, vol. 471, issue 21–22, pp. 1100-1102, Nov 2011, doi:10.1016/j.physc.2011.05.134.

[11] G. K. Williamson, W. H. Hall, "X-ray line broadening from filed aluminium and wolfram", *Acta Metallurgica*, vol. 1, issue 1, pp. 22-31, Jan 1953, doi:10.1016/0001-6160(53)90006-6.

[12] N. T. Mua, C. R. Serrao, Shipra, A. Sundaresan, T. D. Hien and N. K. Man, "High critical current density in Ag-doped Bi-2212 thin films", *Supercond. Sci. Technol.*, vol. 21, no. 10, 105002, July 2008, doi:10.1088/0953-2048/21/10/105002.

[13] A. Sotelo, M. A. Madre, J. C. Diez, Sh Rasekh, L. A. Angurel and E. Martínez, "The influence of Pb and Ag doping on the J_c(H, T) dependence and the mechanical properties of Bi-2212 textured rods", *Supercond. Sci. Technol.*, vol. 22, no. 3, 034012, Feb 2009, doi:10.1088/0953-2048/22/3/034012.

[14] P. Majewski, A. Sotelo, H. Szillat, S. Kaesche, F. Aldinger, "Phase diagram studies in the system Ag-"$Bi_2Sr_2CaCu_2O_8$", *Physica C: Superconductivity*, vol. 275, issue 1–2, pp. 47-51, Feb 1997, doi:10.1016/S0921-4534(96)00686-7.

[15] J. C. Diez, A. Sotelo, S. Rasekh, H. Amaveda, M. A. Torres, P. Bosque, C. Chocarro, M. A. Madre, "Composite Bi-2212/Ag Superconductors Grown by Laser Travelling Floating Zone at Low Rates", *J. Supercond. Nov. Magn.*, vol. 28, pp. 415–418, Feb 2015, doi:10.1007/s10948-014-2758-y.

[16] B. Atilla, I. Ergin, M. Gürsul, B. Özçelik, M. A. Madre, A. Sotelo, "Impact of silver addition on the superconducting performances of $Bi_2Sr_2Ca_{0.925}Na_{0.075}Cu_2O_y$: Ag composite fibers", *Journal of the European Ceramic Society*, vol. 42, issue 14, pp. 6551-6556, Nov 2022, doi:10.1016/j.jeurceramsoc.2022.07.013.

[17] A. Sotelo, M. Mora, M. A. Madre, J. C. Diez, L. A. Angurel, G. F. De la Fuente, "Ag distribution in thick Bi-2212 floating zone textured rods", *Journal of the European Ceramic Society*, vol. 25, issue 12, pp. 2947-2950, 2005, doi:10.1016/j.jeurceramsoc.2005.03.168.

[18] B. Özkurt, M. A. Madre, A. Sotelo, M. E. Yakıncı, B. Özçelik, "Relationship Between Growth Speed, Microstructure, Mechanical and Electrical Properties in Bi-2212/Ag Textured Composites*", J. Supercond. Nov. Magn.*, vol. 25, pp. 799–804, May 2012, doi:10.1007/s10948-011-1346-7.

[19] A. Martinelli, E. Bellingeri, A. Leveratto1, L. Leoncino, C. Ritter, and A. Malagoli, "In situ x-ray and neutron diffraction investigation of Bi-2212 in multifilamentary wires during thermal treatment", *Phys. Rev. Materials*, vol. 2, 084801, Aug 2018, doi:10.1103/PhysRevMaterials.2.084801.

[20] J. K. Shin, S. Ochiai, H. Okuda, Y. Mukai, H. Matsubayashi, S. S. Oh, D. W. Ha, S. C. Kim, M. Sato, "Estimation of Young's modulus, residual strain and intrinsic fracture strain of Bi2212 filaments in Bi2212/Ag/Ag alloy composite wire", *Physica C: Superconductivity*, vol. 468, issue 15–20, pp. 1792-1795, Sep 2008, doi:10.1016/j.physc.2008.05.086.

[21] S. Zhang, C. Li, Q. Hao, J. Feng, T. Lu, P. Zhang, "Optimized Intergrain Connection and Transport Properties of Bi-2212 High-Temperature Superconductors by Ag Nanoparticles Inclusions", *J. Supercond. Nov. Magn.*, vol. 28, pp. 1729–1736, June 2015, doi:10.1007/s10948-015-2981-1.

[22] P. Chen, U. P. Trociewitz, D. S. Davis, E. S. Bosque, D. K. Hilton, Y. Kim, D. V. Abraimov, W. L. Starch, J. Jiang, E. E. Hellstrom and D. C. Larbalestier, "Development of a persistent superconducting joint between Bi-2212/Ag-alloy multifilamentary round wires", *Supercond. Sci. Technol.*, vol. 30, no. 2, 025020, 2017, doi:10.1088/1361-6668/30/2/025020.

[23] D. C. Shin, S.-J. L. Kang, H.-S. Chung, "Dendrite formation in the $Bi_2Sr_2CaCu_2O_8$–Ag system: reactions between Ag and oxide melt", *Physica C: Superconductivity*, vol. 340, issue 2–3, pp. 141-148, Dec 2000, doi:10.1016/S0921-4534(00)00841-8.

[24] B. Özkurt, "Structural, Electric and Magnetic Properties of Bi2Sr2Ag0.03Ca1Cu2Oy Ceramics Modified by Post-annealing", *J. Supercond. Nov. Magn.*, vol. 31, pp. 2459–2464, Aug 2018, doi:10.1007/s10948-017-4509-3.

[25] T.A. Deis, M. Lelovic, N.G. Eror, U. Balachandran, "Effect of Ag doping on structure and critical temperature of Bi2Sr2CaCu2O8+δ superconductors, *Applied Superconductivity*, vol. 6, issue 6, pp. 279-284, June 1998, doi:10.1016/S0964-1807(98)00045-3.